Rev. Adv. Mater. Sci. 31 (2012) 91-99

STATE AND PROCESSES IN GRAIN BOUNDARIES OF Cu SUBJECTED TO SEVERE PLASTIC DEFORMATION

I.V. Alexandrov and R.G. Chembarisova

Department of Physics, Ufa State Aviation Technical University, 12 K. Marx St., Ufa, 450000 Russia

Received: April 20, 2012

Abstract. The states and processes in grain boundaries of Cu, subjected to severe plastic deformation have been analyzed here. It has been shown that microstructure refinement in the process of severe plastic deformation leads to a hyper sensitivity of the processes occurring in the grain boundaries towards the applied hydrostatic pressure. The temperature alterations of the plastic deformation are also followed by activation or suppression of some or other deformation processes in the grain boundaries of Cu in different structure states. These processes are much more intensive in ultra-fine grain states. It has been demonstrated that the temperature decrease, as well as the hydrostatic pressure increase, brings to the growth of stress in the samples. In connection with this, the tendency is more evident in the samples with an ultra-fine grain structure.

1. INTRODUCTION

The recent research has evidently demonstrated the wide opportunities of the severe plastic deformation (SPD) methods for developing the bulk nanostructured states in various metallic materials [1]. The principal SPD methods are the high pressure torsion and the equal-channel angular pressing (ECAP) [1]. The specific microstructure characterized by the developed network of mainly high-angle grain boundaries (GBs) of deformation origin, provides attractive fundamental and functional properties, characteristic for bulk nanostructured materials (BNM) [1,2].

Deformation behavior of BNM is of particular interest, which is characterized by the improved strength characteristics, the absence of strain hardening, the SPD paradox, the high-strain rate and low-temperature superplasticity, the deviations from the Hall-Petch law [3-5]. Thus, it is important to consider the state and the processes in GBs.

The experimentally observed phenomena require additional research and quantitative evaluations of the activity of deformation mechanisms, managing the macroscopic processes. Modeling on the basis of dislocation kinetics equations is one of the most universal approaches to the investigation of the processes, which provides the plastic deformation of materials [6]. Such a modeling allows estimating the dependencies of the flow stress and the average dislocation density from the strain degree for various values of the average grain size, the temperature and the strain rate. The developed models [6-15] are able to describe the most evident effects, concerning the hardening and the ductility of metals in the range from a nanostructured to a coarse-grained (CG) state.

The goal of this paper is the research of the GBs state and their processes by the kinetic modeling method depending on the strain degree, the temperature, the hydrostatic pressure during the SPD,

Corresponding author: I.V. Alexandrov, e-mail: iva@mail.rb.ru

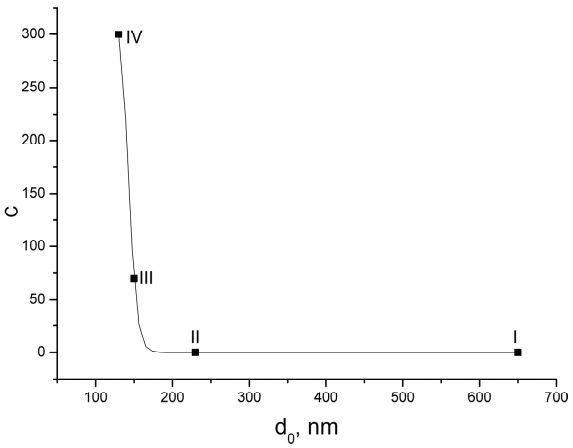

Fig. 1. The model (■) dependency of coefficient *C*, characterizing the speed of generation of deformation vacancies from an average grain size d_0 in the Cu samples, taken in an initial state (I) and after 1st, 4th, and 8th ECAP passes (II, III, IV respectively).

and the effect of GBs on the deformation behavior and hardening of a pure Cu.

2. THE MODELING METHODIC

Presently the concepts about the grain structure and their boundaries are being developed in works of a few authors, for instance [16,17]. However, the universally accepted concepts have been chosen in the model development, which have been used in works of V.V. Rybin [18], M. Zehetbauer [9], Y. Estrin and L.S. Tóth [8,15].

In accordance with the data of experimental observations [18] it has been considered that the structure of the SPD material consists of the fragments of cells, limited by the boundaries from the redundant dislocations, "fluffed up" by the non-redundant sessile dislocations [18]. Such a structure has been called a fragmented one with the size of a fragment *d* [12].

The dislocations in the inner area of a fragment develop the cell structure with the total density of immobilized dislocations in the cell walls and their inner areas equal to ρ_c. Further, the cell block has been determined as the grain of a CG material.

It is difficult to observe the dislocations in UFG materials, as the dislocations emitted by the dislocation sources from GBs disappear in the opposite boundary. Each grain contains only few dislocations [6]. Thus, further the fragment with the inner area almost free from dislocations has been determined as the grain of an UFG material.

The account of the total dislocation density ρ_w and the density of irredundant sessile dislocations ρ_f in GBs allowed calculating the density of redundant dislocations in boundaries, and, thus, the misorientations between the grains.

To explain the absence of strengthening at the stage of the developed plastic deformation, the dislocation annihilation has additionally been considered during their non-conservative movement, caused by the vacancy diffusion, the annihilation of edge dislocations of the opposite sign. The material flow has also been suggested to be maintained among the others by the dislocation multiplication at a multiple cross slip. In the result the modeling equations have been received, which describe the dislocation density evolution in time *t* in GBs and the inner grain areas in a common case [12,15]:

$$\dot{\rho}_w = \frac{6P_f\beta^*\dot{\gamma}_w^r\left(1-f\right)^{2/3}}{bdf} + \frac{\sqrt{3}\beta^*\dot{\gamma}_w^r\left(1-f\right)\sqrt{\rho_w}}{fb} + \frac{\delta_f\rho_f^{1/2}\dot{\gamma}_w^r}{b} - \frac{\delta_a\rho_w\dot{\gamma}_w^r}{b} - \frac{R_f\rho_f\dot{\gamma}_w^r}{b} - 2B'\rho_f^3, \quad (1)$$

where P_f is the share of immobilized dislocations, $\dot{\gamma}_w^r$ is the resolved strain rate in GBs, *f* is the volume share of the fragment boundaries, δ_f is the multiplication coefficient on the forest dislocations, the density of which is equal to ρ_f, $\delta_f \approx 10^{-2}$ [14]. $d = K/\sqrt{\rho_{total}}$ is the average grain size, ρ_{total} is the average dislocation density, *K* is the constant of proportionality [15], β^* is the efficiency coefficient of dislocation sink into boundaries [15], *b* is the value of the Burgers vector, $k_a = \delta_a/b = k_0(\dot{\gamma}_w^r/\dot{\gamma}_0)^{-1/n}$ is the annihilation coefficient during the double cross slip, where the parameter k_0 characterizes the intensity of annihilation processes at temperature *T* = 0K, and *n* is their sensitivity to the strain rate at the cross slip. The value *n* grows along with the increase of the stacking fault energy and depends, like the value *m* reflecting the sensitivity on the strain rate, inversely proportional to *T* [19].

In the model, according to the work [20] it has been considered that annihilation of edge dislocations of the opposite sign takes place at the distances less than the dislocation annihilation length R_f, equal to 1.6 nm.

The dislocation density evolution in time in the inner areas of fragments happens according to the law

$$\dot{\rho}_c = \frac{\alpha^*\dot{\gamma}_c^r\sqrt{\rho_w}}{\sqrt{3}b} + \frac{\delta_f\rho_c^{1/2}\dot{\gamma}_c^r}{b} - \frac{6\beta^*\dot{\gamma}_c^r}{bd\left(1-f\right)^{1/3}} - \frac{\delta_a\rho_c\dot{\gamma}_c^r}{b}, \quad (2)$$

where α^* is the efficiency coefficient of the Frank-Read sources [15], $\dot{\gamma}_c^r$ is resolved strain rate in the inner areas of fragments.

The density of non-redundant sessile dislocations in fragment boundaries changes with time according to the law:

$$\dot{\rho}_f = \left(\frac{6P_f \beta^* \dot{\gamma}_w^r \left(1-f\right)^{2/3}}{bdf} + \frac{\sqrt{3}\beta^* \dot{\gamma}_w^r \left(1-f\right)\sqrt{\rho_w}}{fb} + \frac{\delta_f \rho_f^{1/2} \dot{\gamma}_w^r}{b} \right) P_f' - \frac{R_f \rho_f \dot{\gamma}_w^r}{b} - 2B' r_f^3, \quad (3)$$

where P_f' is the share of forest dislocations out of the whole number of dislocations, entered into the fragment boundaries.

In connection with this, the total dislocation density is

$$\rho_{total} = f\rho_w + \left(1-f\right)\rho_c, \quad (4)$$

where the volume share of the GBs *f* with the thickness *w* is determined as [21]:

$$f = \frac{d^3 - \left(d-w\right)^3}{d^3}. \quad (5)$$

In work [22] the analytical dependency of the volume share of GBs *f* from the-resolved strain has been received in the result of generalization of experimental data

$$f = f_\infty + \left(f_0 - f_\infty\right)\exp\left(-\gamma^r / \tilde{\gamma}^r\right), \quad (6)$$

where f_0, f_∞ - the initial and the ultimate values of the volume share of GBs, $\tilde{\gamma}^r$ is the parameter, characterizing the rate of the value *f* change, depending on the resolved strain γ^r.

The resolved shear stresses τ_w^r and τ_c^r in boundaries and inner areas of the grains are calculated, taking into consideration the corresponding dislocation densities ρ_w and ρ_c [8]:

$$\tau_w^r = \alpha Gb\sqrt{\rho_w}\left(\frac{\dot{\gamma}_w^r}{\dot{\gamma}_0}\right)^{1/m}, \quad (7)$$

$$\tau_c^r = \alpha Gb\sqrt{\rho_c}\left(\frac{\dot{\gamma}_c^r}{\dot{\gamma}_0}\right)^{1/m}, \quad (8)$$

where *G* is the shear modulus, $\dot{\gamma}_0$ is the pre-exponential factor, α is the constant, reflecting the interactions between dislocations.

The deformation behavior of the composite can be determined by the resolved stress τ^r connected with the resolved stresses τ_w^r and τ_c^r according to the rule

$$\tau^r = f\tau_w^r + \left(1-f\right)\tau_c^r. \quad (9)$$

To realize the compatibility conditions of boundaries and inner areas of the grains, it has been assigned that $\dot{\gamma}_w^r = \dot{\gamma}_c^r = \dot{\gamma}^r$.

According to work [23], the dislocation density in the result of their non-conservative movement is decreasing according to the law

$$\frac{d\rho_w^-}{dt} = -\phi'\rho_f^3 = -2B'\rho_f^3, \quad (10)$$

where

$$B' = \sqrt{2}/\left[\pi\left(1-\nu\right)\right]D_c \cdot q_c\left(G\Omega/kT\right),$$
$$D_c = D_\infty \cdot C_V \cdot \exp\left(-H_c^m/kT\right). \quad (11)$$

C_V is the vacancy concentration, developing during deformation, H^m_c is the enthalpy of vacancy migration activation along the dislocation cores [9], Ω is the atomic volume, q_c is the cross-sectional area of a dislocation core, D_c is the diffusion coefficient along the dislocation core, multiplier D_{c0} is assumed in correspondence with the literature data [9], n is the Poisson's ratio.

Passing in Eq. (10) from the variable *t* on to variable γ^r, one can set up a dependency of function $\phi = \phi'/\dot{\gamma}^r$ on $d\rho_w/d\gamma^r$, under the condition that ϕ is proportional to the concentration of vacancies C_v. At the first approximation the concentration of vacancies (function ϕ) is considered to depend linearly on the strain γ^r with the proportionality coefficient *C*, that is why it is possible to write

$$\phi\left(\left.\frac{d\rho_w}{d\gamma^r}\right|_{t+1}\right) = \phi\left(\left.\frac{d\rho_w}{d\gamma^r}\right|_t\right) + \left.\frac{d\rho_w}{d\gamma^r}\right|_t C\, d\gamma^r. \quad (12)$$

The density of the non-redundant sessile dislocations ρ_f, comprising the part of the dislocation density in the GBs ρ_w, changes during their non-conservative motion of dislocations according to the law (10). Comparing the corresponding annihilation component in Eq. (10) with its right part, we get $\phi' = 2BC_v$, where $B = B'/C_v$. Herein, the vacancy concentration depending on the strain can be determined from the expression

$$C_v = \phi'/2B. \quad (13)$$

The model allows calculating the misorientations between the neighboring grains, which has been demonstrated in work [12].

The kinetic parameters of the model have been determined by the method of successive approximations by fixing the characteristic points on the experimental curve "the true stress – the true strain". Thus, the number of points corresponds to the number of the determined parameters. The affect of every kinetic parameter on the flow stress value has been studied here.

To consider the effect of the crystallographic texture, the values of the resolved strain rate $\dot{\gamma}_s^r$ in each slip system in the grain have been obtained with the help of a visco-plastic self-consistent (VPSC) model [24]. The data obtained in the end of modeling of each succeeding ECAP pass have been used as the input parameters during the modeling of a previous ECAP pass. According to the received values of the volume ratios V_i and the resolved strain rates $\dot{\gamma}_s^r$ in every slip system the Taylor factors have been calculated at every deformation step [8,12].

The developed model [12,15] has allowed describing the dislocation density evolution quantitatively in the samples, subjected to the ECAP.

3. MODELING RESULTS AND THEIR DISCUSSION

Let's view the results of the analysis of strain degree effect (the grain size), temperature and hydrostatic pressure on the states and processes in GBs during the SPD.

3.1. The influence of the SPD degree (the grain size)

In the process of modeling the experimental data obtained in IPAM USATU have been used. The experimental details are described in [12]. The Cu samples of 99.9% purity annealed at temperature 550 °C for 1 hour (the initial state) and Cu after the 1st, 4th, and 8th ECAP passes along the route B_c [1] have been investigated.

According to the modeling results, the dislocation density in GBs increases along with the growth of the strain degree during the tensile deformation of Cu in an initial state and after the 1st ECAP pass. In the process of tensile deformation of the samples after the 4th and the 8th ECAP passes the dislocation density increase in GBs changes to the tendency towards the saturation state. Thus, in the samples subjected to the ECAP the dislocation density in GBs increases along with the number of passes.

The modeling results have shown that after the 8th ECAP pass the role of the annihilation processes in GBs, conditioned by the non-conservative movement of the edge dislocations, is decreasing. This fact is proved by the increase of parameter *C* (see the Eq. 13), which characterizes the speed of the increase of deformation vacancies (Fig. 1). The model has allowed forecasting the evolution of the vacancy concentration in GBs and estimating their role in strain hardening and the behavior of the developing GBs. It has been demonstrated that a catastrophic increase of the vacancy concentration takes place along with the increase of the number of passes [12]. Herein, the concentration of the deformation vacancies grows along with the plastic strain degree. However, during the deformation of the samples after the 4th and the 8th ECAP passes the increase of the vacancy concentration is limited and aims for the saturation state along with the increase of the plastic strain degree, which is followed by the limitation of the dislocation density increase in GBs in the result of annihilation intensification during the non-conservative dislocation movement [11]. Actually, at the initial moment of deformation of the samples the dislocation density increases. The concentration of deformation vacancies is increasing too. The increase of the vacancy concentration leads to the reduction of the forest dislocation density. The decrease of the forest dislocation density is followed by the limitation of dislocation annihilation during the non-conservative movement and dislocation density increase in GBs. At the same time, the concentration of deformation vacancies continues growing, without aiming for the saturation state during the deformation of the samples in the initial state and after the 1st ECAP pass. The dislocation density increases here too [12].

The obtained modeling results agree with the well-known experimental data [9,25,26] and modeling results [9,25]. In work [25] the modeling data have brought to the conclusion that the concentration of deformation vacancies is increasing along with the pressure increase during the torsion of the Cu samples. In connection with this, the results agree with the experimental data in the process of SPD. The less is the grain, the higher it is. Nowadays there are some experimental data about the concentration of deformation vacancies after four ECAP passes [26]. According to the received results, the concentration achieves the value about 3.5×10^{-4}.

The modeling results of evolution of concentration of deformation vacancies in the process of deformation of Cu samples in various structural states [12] agree with the data containing in the works

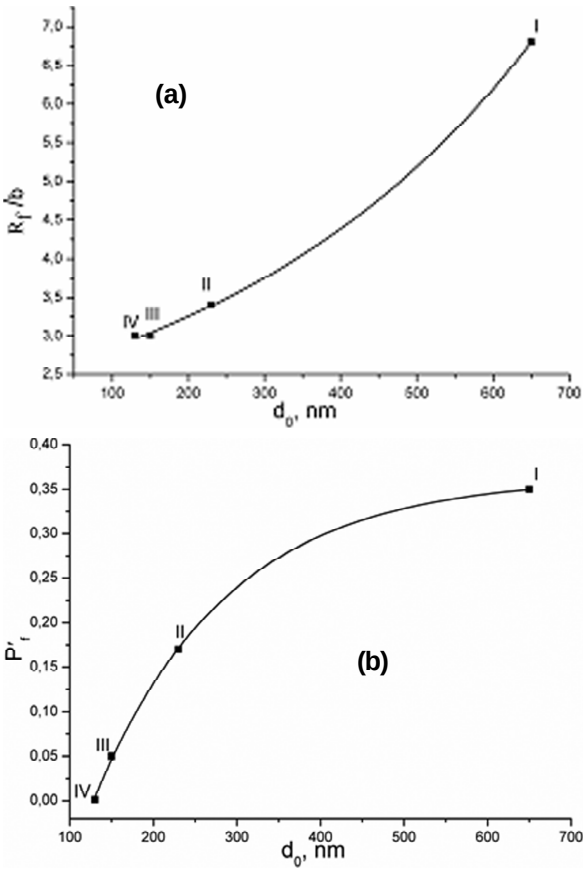

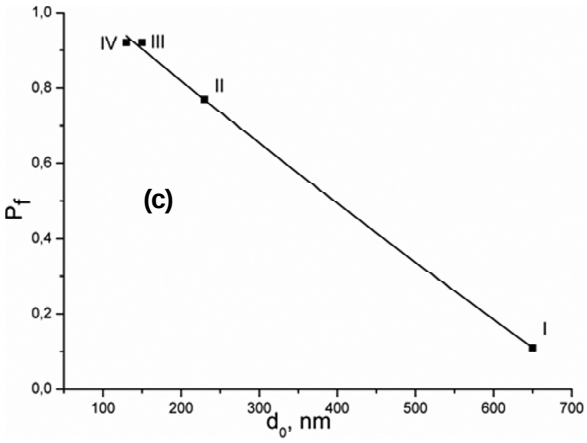

Fig. 2. The model (■) dependencies of the annihilation coefficient R_f of the dislocations of the opposite sign (a), the shares of non-redundant sessile dislocations in GBs P_f' (b), the shares P_f of dislocations immobilized into GBs (c) from the average grain size d_0, formed in the initial state (I) and in states after the 1st, the 4th, and the 8th ECAP passes (II, III, IV) respectively.

mentioned above. In work [27] it has been demonstrated that the model allows predicting the values of concentrations of deformation vacancies, which agree according to the order of the value with the experimental data. No doubt, the further experimental research is required to determine the concentration of deformation vacancies developed during the tensile deformation of the Cu samples, subjected to the different number of the ECAP passes.

The decrease of the forest dislocation density in GBs brings to the limitation of dislocation annihilation during their capture, which can be related to the decrease of annihilation dislocation possibility (Fig. 2a). Thus, the parameter R_f/b is decreasing along with the decrease of the grain size. In connection with this, the mechanism of dislocation multiplication on the "forest" dislocations is suppressed (the third addend in the equation is annihilated (1)). The pointed out changes reflect the quantitative modifications in the structure of GBs with the grain size decrease. In the process of the 4th ECAP pass the inconsiderable structure refinement together with the GBs improvement takes place [12]. The misorientations between the grains are decreasing on the back of their almost frozen sizes [12]. The structure refinement takes place mainly up to the 4th ECAP pass [12], but, in connection with this, the misorientations between the fragments stay small. The obtained results agree with the experimental data, which are reduced in work [28].

While the number of ECAP passes is increasing, the GBs become more ordered (the density of the "forest" dislocations ρ_t is decreasing, the share of non-redundant sessile dislocations P_f' is negligibly small (Fig. 2b). Parameter P_f', reflecting the share of irredundant sessile dislocations in GBs after the 8th ECAP pass is decreasing 350-fold in comparison with its value for Cu, taken in an initial state. After the 8th ECAP pass the share of dislocations moving into the range of non-redundant sessile ones, is 50 times less than after the 4th ECAP pass. Thus, the density of the non-redundant sessile dislocations is decreasing sharply. Correspondingly the annihilation of dislocations during grip in boundaries and the dislocation multiplication on the "forest" dislocations become more difficult. Undoubtedly, the experimental research to determine the densities of the dislocations of different types, developed during the tensile deformation of Cu samples, subjected to the different number of the ECAP passes are required here. However, the data obtained in the result of modeling about an average dislocation density agree with the experimental data, as it has been shown in work [12].

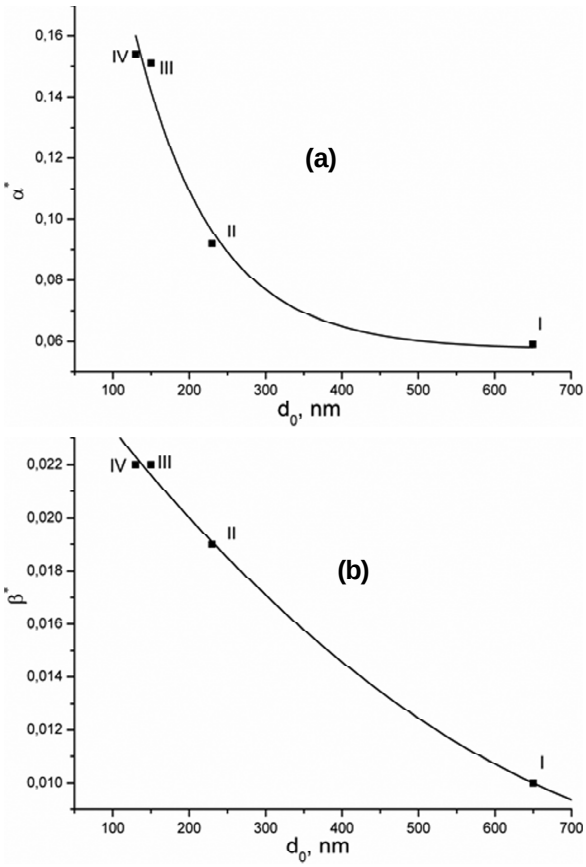

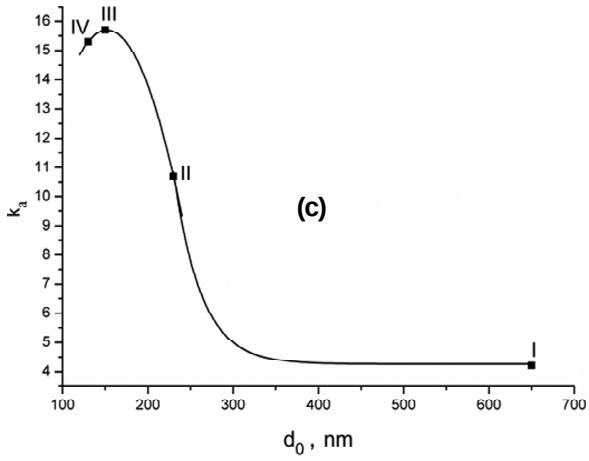

Fig. 3. The model (■) dependencies of coefficient α^*, characterizing the efficiency of the Frank-Read sources (a), coefficient α^*, characterizing the efficiency of GBs, as the dislocation sinks (b) and annihilation coefficient of the screw dislocation at the double cross slip k_a (c) from the average grain size d_0, developed in the initial state after the 1st, the 4th and the 8th ECAP passes (II, III, IV), respectively.

After the 4th ECAP pass the GBs become almost impenetrable. Indeed, the parameter P_f characterizing the share of immobilized dislocations into GBs is increasing along with the degree of accumulated strain, and after the 4th ECAP pass remains unchanged achieving the value close to 1 (Fig. 2c). Thus, the value of the parameter after the 8th ECAP pass is approximately 8.4 times higher than its value for Cu in the initial state.

The dislocation density in the GBs and the total dislocation density are increasing along with the decrease of an average grain size (with the increase of the number of ECAP passes). An inconsiderable strain hardening of materials, subjected to the ECAP, can be explained by the fact that the activity increase of the sources (Fig. 3a) and the sinks (Fig. 3b) is compensated by the increase of annihilation processes (Figs. 1 and 3c). The contribution of each of them can be estimated.

3.2. Effect of temperature

The analysis of GBs state depending on the deformation temperature during the tensile deformation of an UFG Cu with the average grain size equal to 300 nm, obtained by the ECAP method [4] and initial CG Cu with the grain size d = 18 μm [29] at temperatures 77K and 298K has been fulfilled. On the basis of the kinetic modeling results [30] it has been have been shown that temperature has a weak influence on the dislocation density in the inner grain areas, while in GBs the pointed out dependency on the temperature is significant, especially in an UFG Cu.

Annihilation during the non-conservative dislocation motion which is characterized by the coefficient C in the UFG Cu takes place much more intensive, than in the CG Cu. Herein, the temperature increase significantly strengthens this process (Table 1).

The temperature increase also intensifies the annihilation during the cross slip, which is much more expressed in the UFG Cu (Table 1). The enforcement of annihilation processes in GBs in the UFG Cu with the temperature increase speaks for the developing the dynamic recovery at room temperature and material strengthening at cryogenic temperature.

As it follows from [30] the temperature decrease has a favorable effect on the process of grain refinement and development of high-angle GBs in the UFG Cu. The latest one is related to the decrease of the share of irredundant sessile dislocations P_f' in GBs (Table 1).

Table 1. The values of the model parameters.

Parameter	CG	Cu	UFG	Cu
T, K	77	300	77	300
α^*	6.57×10^{-2}	6.87×10^{-2}	5.8×10^{-2}	0.105
α^*	8.6×10^{-3}	9.16×10^{-3}	1.76×10^{-2}	3.08×10^{-2}
k_0	3.2	3.96	11.15	21.59
P_f'	3.9×10^{-1}	0.40	1.816×10^{-4}	4.156×10^{-4}
C_v	4.77×10^{-7}	1.085×10^{-6}	89.006×10^{-4}	300.0

Table 2. The values of the parameters, obtained in the result of HPT modeling at various values of a hydrostatic pressure.

Parameter	P = 0.0 GPa	P = 5.0 GPa
P_f'	0.35	0.08
C	3.4×10^{-6}	8.1×10^{-6}
α^*	0.061	0.154
α^*	0.006	0.019
k_a	4.0	15.3
K	10.0	7.0
P_f	0.11	0.92

At room temperature the activity of the Frank-Read sources (the parameter α^*), located in GBs of the UFG Cu, is higher than in a CG state. At the same time the temperature decrease brings to their loss of activity in the UFG Cu in comparison with the CG Cu (Table 1). The efficiency of GBs as the dislocation sinks (parameter β^*), is higher in an UFG Cu in comparison with a CG Cu, thus, it is increasing along with the temperature growth (Table 1).

3.3. The effect of the hydrostatic pressure

The value of the applied hydrostatic pressure is one of the most important SPD parameters, influencing the microstructure evolution, the deformation mechanisms, states and processes in GBs [25]. Let's analyze the effect of this parameter on the state and processes in GBs, founding on the results of kinetic modeling [27] and experimental investigations [25]. The samples of a pure Cu have been taken as the research objects, which have been subjected to the high pressure torsion under the atmosphere pressure and under the pressure 5.0 GPa, typical for the SPD process. The samples have been deformed at room temperature. The resolved shear strain has been $\gamma^r = 90$. The rate of the high pressure torsion has been $\dot{\gamma}^r \approx 10^{-2}$ s^{-1}.

According to the modeling results the dislocation density in GBs during the HPT of the Cu samples under pressure 5.0 GPa is 1.7 times higher than during the torsion under the atmosphere pressure at the same strain degree $\gamma^r = 90$. Thus, the evolution of the total dislocation density in the both cases agrees with the experimental data, obtained by the authors of the papers [9, 25].

The share of the non-redundant dislocations P_f' decreases along with the hydrostatic pressure increase (Table 2). In connection with this, the density of the non-redundant sessile dislocations is higher at the HPT and increases with the growth of the strain degree [27]. This speaks for the limitation of dislocation annihilation during their non-conservative motion, which is followed by the increase of vacancy concentration and dislocation density in GBs [27].

The SPD leads to the development of the great many of deformation vacancies. The concentration of vacancies reveals the catastrophic growth along with the hydrostatic pressure increase [27]. If an equilibrium concentration of the thermal vacancies at room temperature has an order $C_v \approx 10^{-20}$ [25], the concentration of deformation vacancies increases to the 15th order during the HPT under pressure 5.0 GPa, while during the torsion under the atmosphere pressure it is 8 orders higher at the strain degree $\gamma = 25$, which agrees with the results of work [31].

Parameter C, which controls the intensity of deformation vacancy concentration, is increasing with the hydrostatic pressure growth (Table 2). Consequently, the diffusion processes in GBs are slowing down. Thus, the annihilation during the non-conservative dislocation motion is limited, which brings to the growth of the flow stress. However, during the following development of the samples the increase of deformation vacancy concentration is limited, and it aims for the saturated state. This, in its turn, leads to the limitation of the density increase of non-redundant sessile dislocations in GBs, hence, to the dislocation density in GBs [27].

The decrease of the density of non-redundant sessile dislocations at a simultaneous growth of the total dislocation density in GBs brings to the misorientation growth between the neighboring grains (Fig. 4 in [27]). Thus, their sizes are decreasing along with the torsion pressure, as well as with the strain degree increase, and they aim for a certain saturated condition [27].

The hydrostatic pressure, as it follows from the obtained modeling results, intensifies the processes of dislocation multiplication. This is proved by the fact that the activity of the sources, characterized by the parameter α^* in GBs is increasing, while the hydrostatic pressure is growing too (Table 2).

The GBs are not only the sources, but they are the sinks for the dislocations. Herein, the efficiency of the sinks, characterized by the parameter β^*, is increasing along with the growth of a hydrostatic pressure (Table 2).

In accordance with the modeling results the high pressure torsion brings to the intensification of annihilation processes in ~3.8 times during the double cross slip. Thus, the parameter k_0 is the coefficient of dislocation annihilation at temperature T=0K in the expression for the annihilation coefficient $k_a=\delta_a/b$, characterizing the annihilation during the cross slip higher at HPT 5.0 GPa than while the torsion at atmosphere pressure (Table 2).

The torsion pressure increase contributes into the structure refinement as well. This is proved by the fact that parameter K, characterizing the grain sizes is decreasing (Table 2).

Parameter P_f', characterizing the share of immobilized into GBs dislocations, is increasing along with the growth of pressure torsion. Consequently, the GBs become almost impenetrable at high pressure torsions (Table 2).

4. CONCLUSIONS

According to the results of kinetic modeling, carried out within the developed dislocation model, considering the wholeness of all the possible deformation mechanisms and presenting the development of the well-known composite models, the quantitative evaluations of the state and processes in the GBs of Cu, subjected to the SPD, have been made. It has been demonstrated that in the process of SPD, followed by the microstructure refinement, the processes occurring in GBs of Cu are sensitive to the applied hydrostatic pressure. The temperature alteration of the plastic deformation brings to the activation or suppression of some deformation processes in GBs of Cu with different microstructure, both the CG and obtained in the process of SPD. Herein, these processes are more intensive in case of UFG states of Cu, obtained by the SPD method.

On the one hand, the temperature increase as well as the hydrostatic pressure growth activates the work of the Frank-Read sources. The efficiency of GBs as the sinks for dislocations is increasing. Both the annihilation of the screw dislocations during their double cross slip and their annihilation during the non-conservative motion are increasing. Thus, these processes are more intensive in the UFG Cu. Simultaneously, on the other hand, the same effects can be observed in the process of hydrostatic pressure increase and the temperature decrease. For instance, the concentration of the deformation vacancies shows a considerable growth. The same factors influence favorably the structure refining and the increase of misorientations between the grains. The last one is connected with the reduction of the share of non-redundant sessile dislocations in the GBs. Thus, the share of the immobilized into GBs dislocations is increasing as well and they become almost impenetrable.

The most sensitive to the temperature and hydrostatic pressure alterations characteristic is the dislocation density in GBs of an UFG Cu. Both the temperature reduction and the hydrostatic pressure increase bring to its growth. Thus, the total dislocation density increases too. In the result the flow stress of Cu is increasing as well.

REFERENCES

[1] R.Z. Valiev, R.K. Islamgaliev and I.V. Alexandrov // *Progr. Mater. Sci*. **45** (2000) 103.
[2] R.Z. Valiev and R.K. Islamgaliev // *Phys. Met. Metallogr*. **85(3) (**1998) 367.
[3] R.Z. Valiev, I.V. Alexandrov, Y.T. Zhu and T.C. Lowe // *J. Mater. Res*. **17(1)** (2002) 5.
[4] G.T. Gray III, T.C. Lowe, C.M. Cady, R.Z. Valiev and I.V. Aleksandrov // *NanoStr. Mater*. **9** (1997) 477.
[5] I.P. Semenova, G.Kh. Salimgareeva, V.V. Latysh, T. Lowe and R.Z. Valiev // *Mater. Sci. Ing. A* **503** (2009) 92.
[6] G. A. Malygin // *Phys. Solid. State* **49** (2007)1013.
[7] Y. Estrin and H. Mecking // *Acta Metall. Mater*. **32(1)** (1984) 57.
[8] Y. Estrin, L.S. Tóth, A. Molinari and Y. Bréchet // *Acta Mater*. **46** (1998) 5509.
[9] M. Zehetbauer // *Acta mater.* **41** (1993) 589.

[10] P. Les and M. Zehetbauer // *Key Eng. Mater.* **97-98** (1994) 335.
[11] M. Zehetbauer and V. Seumer // *Acta metall. mater.* **41(2)** (1993) 577.
[12] I.V. Alexandrov and R.G. Chembarisova // *Rev. Adv. Mater. Sci.* **16(1/2)** (2007) 51.
[13] I.V. Alexandrov and R.G. Chembarisova // *Mater. Sci. Forum* **667-669** (2011) 749.
[14] I.V. Alexandrov, R.G. Chembarisova, V.D. Sitdikov and V.U. Kazyhanov // *Mater. Sci. Eng. Ŕ* **493** (2008) 170.
[15] L.S. Tóth, A. Molinari and Y. Estrin // *J. Eng. Mater. Technol.* **124** (2002) 71.
[16] V.N.Chuvildeev and V.I. Kopylov, *Deformation and Fracture of Materials and Nanomaterials: the Sourcebook of the IVth International Conference DFMN 2011, October, the 25-28th, 2011* (Moscow, 2011), p. 219.
[17] Y.S. Nechaev, *Deformation and Fracture of Materials and Nanomaterials: the Sourcebook of the IVth International Conference DFMN 2011, October, the 25-28th, 2011* (Moscow, 2011), p. 193.
[18] V.V. Rybin, *Large Plastic Deformations and Metal Fracture* (Metallurgy, Moscow, 1986).
[19] G.A. Malygin // *Solid State Physics* **34** ą 10 (1992) 3200.
[20] U. Essman and H. Mughrabi // *Phil. Mag. A* **40** (1979) 731.
[21] R.Z. Valiev and I.V. Alexandrov, *Nanostructured Materials, Obtained by the severe Plastic Deformation* (Logos, Moscow, 2000).
[22] S. Kok, A.J. Beaudoin and D.A. Tortorelly // *Acta Mater*. **50** (2002) 1653.
[23] F.B. Prinz and A.S. Argon // *Acta metall. mater.* **32(7)** (1984) 1021.
[24] C.N. Tomé // *Mod. Sim. Mats. Sci. Eng*. **7** (1999) 723.
[25] M.J. Zehetbauer, H.P. Stüwe, A. Vorhauer, E. Schafler and J. Kohout // *Adv. Eng. Mat.* **5(5)** (2003) 330.
[26] E. Schafler, A. Dubravina and Z. Covacs , In: *The Minerals, Metals & Materials Society: Proc. of the 2nd Int. Symposium Ultrafine Grained Materials, 2002 TMS Annual Meeting, Seattle, USA, Feb. 17-21, 2002* (Warrendale, 2002), p. 605.
[27] I.V. Alexandrov, R.G. Chembarisova and V.D. Sitdikov. // *Materials Science & Engineering A* **463** (2007) 27.
[28] R.Z. Valiev and T.G. Langdon // *Prog. Mater. Sci*. **51 (**2006) 881.
[29] H. Conrad // *Mater. Sci. Eng. A* **341** (2003) 216.
[30] I.V. Alexandrov and R.G. Chembarisova // *Phys. Met. Metallogr*. **110** (2010) 70.
[31] M.J. Zehetbauer, G. Steiner, E. Schafler, A. Korznikov and E. Korznikova // *Mater. Sci. Forum* **503-504** (2006) 57.